Variability of snow and rainfall partitioning into evapotranspiration and summer runoff across nine mountainous catchments

Matthias Sprenger[1*], Rosemary W.H. Carroll[2], James Dennedy-Frank[1], Erica R. Siirila-Woodburn[1], Michelle E. Newcomer[1], Wendy Brown[3], Alexander Newman[3], Curtis Beutler[3], Markus Bill[1], Susan S. Hubbard[4], Kenneth H. Williams[1,3]

[1]Lawrence Berkeley National Laboratory, Berkeley, CA, USA

[2]Desert Research Institute, Reno, NV, USA

[3]Rocky Mountain Biological Laboratory, Crested Butte, CO, USA

[4]Oak Ridge National Laboratory, Oak Ridge, TN, USA

*Corresponding author: msprenger@lbl.gov

Key points:

1.) For the mountainous catchments in the Upper Colorado River, the fate of snow (rain) is 33% (67%) ET and 13% (8%) summer streamflow.
2.) In catchments with relatively higher tree density, snow was more likely to evapotranspire with less rain and snow sustaining streamflow.
3.) Increased rainfall led to greater share of rain in evapotranspiration rather than streamflow, while snowfall variation had little effect.

Abstract

Understanding the partitioning of snow and rain contributing to either catchment streamflow or evapotranspiration (ET) is of critical relevance for water management in response to climate change. To investigate this partitioning, we use endmember splitting and mixing analyses based on stable isotope (^{18}O) data from nine headwater catchments in the East River, Colorado. Our results show that one third of the snow partitions to ET and 13% of the snowmelt sustains summer streamflow. Only 8% of the rainfall contributes to the summer streamflow, because most of the rain (67%) partitions to ET. The spatial variability of precipitation partitioning is mainly driven by aspect and tree density across the sub-catchments. Catchments with higher tree density have a higher share of snow becoming ET, resulting in less snow in summer streamflow. Summer streamflow did not contain more rain with higher rainfall sums, but more rain was taken up in ET.

Plain language summary

Snowmelt from the Rocky Mountains is crucial for the water supply in the Upper Colorado River Basin (UCRB). With reduced snowpack and earlier snowmelt due to climate change, it is important to understand how much of the snow directly contributes to streamflow and how much returns directly to the atmosphere via evaporation and vegetation use, called evapotranspiration. We applied a stable isotope mass balance approach to investigate this for nine catchments in the UCRB. We found that snow sustains not only most the streamflow but also ¾ of the evapotranspiration. Rainfall was mostly (2/3) lost to the atmosphere through evapotranspiration. The variation of the snow and rain contributions to streamflow and evapotranspiration were mainly driven by the catchment aspect and tree density. The findings show that the timing of snowmelt (influenced by aspect) and plant water use (influenced by tree density) determined how much snow became streamflow and evapotranspiration.

1 Introduction

Mountainous systems are among the most sensitive environments to a warming climate because of shifts that occur when snowfall is reduced and snowmelt takes place earlier due to higher temperatures (Hock et al., 2019). Such changes are already observed (e.g., Musselman et al., 2021) and have been further projected (e.g., Ikeda et al., 2021) for the Rocky Mountains. It is crucial to understand how snow and rain impact the runoff (Q) and evapotranspiration (ET) dynamics because of their role in sustaining the water supply in downstream regions (Immerzeel et al., 2020). Inter-seasonal storage transfer is an important process that needs to be well understood to account for its potential impacts on ecosystem and anthropogenic water supply due to the interplay of a highly seasonal water input during snowmelt, the resulting hydrograph peak, and the strong seasonality of ET fluxes Disentangling how snow and rain partition into Q and ET is critical for understanding potential ramifications of a low-snow to no-snow future (Woodburn et al., 2021).

While snow is recognized as a key source for the water supply in the Western US (Li et al., 2017), the relative share of snow versus rain in sustaining vegetation (i.e., ET) and the relative fraction of snow and rain becoming Q and ET remains currently unclear. Tracer approaches which can track the fate of rain and snow in mountainous hydrological systems can fill this gap. A strong difference in the stable isotope ratios (^{2}H and ^{18}O) of snowfall and rainfall enables isotope-based endmember mixing and splitting analyses (Kirchner and Allen, 2020) to derive the relative share of these inputs in the Q and ET fluxes (i.e., “mixing”), as well as partitioning of the inputs into Q and ET (i.e., “splitting”). Here, we apply such isotope mass balance analyses for nine headwater catchments in the East River, Colorado to address how the partitioning of snow and rain into summer runoff and ET vary across headwater catchments of contrasting landscape characteristics and in response to meteorological variation.

2 Methods

2.1 Study sites and data

Our study took place in the East River Watershed and the Coal Creek catchment in the Upper Colorado River Basin (UCRB) (Hubbard et al., 2018). The lithology of the main stem East River Watershed is dominated by Cretaceous Mancos shale bedrock with Oligocene quartz monzonite and granodiorite laccoliths comprising many of the higher elevation peaks. At Coal Creek, the underlying bedrock is mainly composed of Cretaceous and Eocene sandstones, mudstones, and quartz monzonite and granodiorite intrusive rocks (Gaskill et al., 1991; Uhlemann et al., 2022). The climate in the region is defined as continental subarctic with long, cold winters and short, cool summers (Dfc, according to Koeppen-Geiger, Peel et al., 2007)). Due to the large elevation gradient from 2600 to 4380 m a.s.l., meteorological conditions vary strongly within the catchments. Based on the two SNOTEL sites within the East River, Schofield at 3,261 m a.s.l. and Butte at 3,097 m a.s.l., the average daily air temperature ranges between -8.3°C in December to 11°C in June at the lower-elevation site with about 1.6°C colder temperatures at the high-elevation site (Carroll et al., 2018). Precipitation is dominated by snow, accounting for about 70% of precipitation at Schofield and 66% at Butte. However, annual average precipitation is almost double at the higher Schofield site (1,200 ± 233 mm/year) compared to the lower- elevation site Butte (670 ± 120 mm/year) SNOTEL site (Carroll et al., 2018).

Our study includes eight sub-catchments from the East River Watershed as defined in Figure 1, as well as the Coal Creek catchment. Catchment characteristics vary greatly in their size; average slope; aspect; average elevation; relief; drainage density; topographic wetness index; tree density; their share of montane, subalpine, upper subalpine, and alpine life zones; and their share of Mancos shale or barren land (Suppl. Table 1). Dominant forest cover in the study region is conifer (Spruce-Fir and Lodgepole Pine) and to lesser extent aspen forest (about 10% of area). With elevation, grass and forb cover increases, and above 3700 m barren land, defined as rocky outcrops and sparse vegetation, dominates. The catchment areas range between 2.55 and 85 km^2. The dominant aspect for the western sub-catchments is east, while the eastern sub-catchments are primarily southwest. Average catchment elevation ranges between 3,148 and 3,513 m a.s.l. and the relief is between 904 and 1,362 m (Suppl. Table 1).

We measured streamflow at each catchment outlet (Carroll et al., 2020a; Carroll and Willlams, 2019) and filled gaps that occurred based on a machine learning approach described in the supplementary material (Text S1, Newcomer et al., 2022). Since water year 2015, we sampled the stream water through automatic samplers (Model 3700; Teledyne ISCO, NE, USA) at the Pumphouse and Coal Creek locations at daily to fortnightly frequency and via manual sampling at the other catchment outflows on weekly to twice monthly frequency (Williams et al., 2020). Precipitation was sampled on event basis in the water years 2015 and 2016 and quantified as snow or rain (Carroll et al., 2021). To prevent fractionation prior to sample retrieval, bottles were pre-filled with 2-cm mineral oil to serve as a barrier to evaporation. All samples were filtered through 0.45-µm Polyvinylidene difluoride (PVDF) membrane filters (EMD Millipore Corp.) into 2-mL septa-capped glass vials and refrigerated until analysis. We measured the isotope ratios of water (^2H & ^{18}O) via off-axis integrated cavity output spectrometry (Picarro L2130-i or Los Gatos Research Liquid Water Isotope Analyzer (LWIA)) and report all isotope ratios in δ-notation relative to the Vienna Standard Mean Ocean Water.

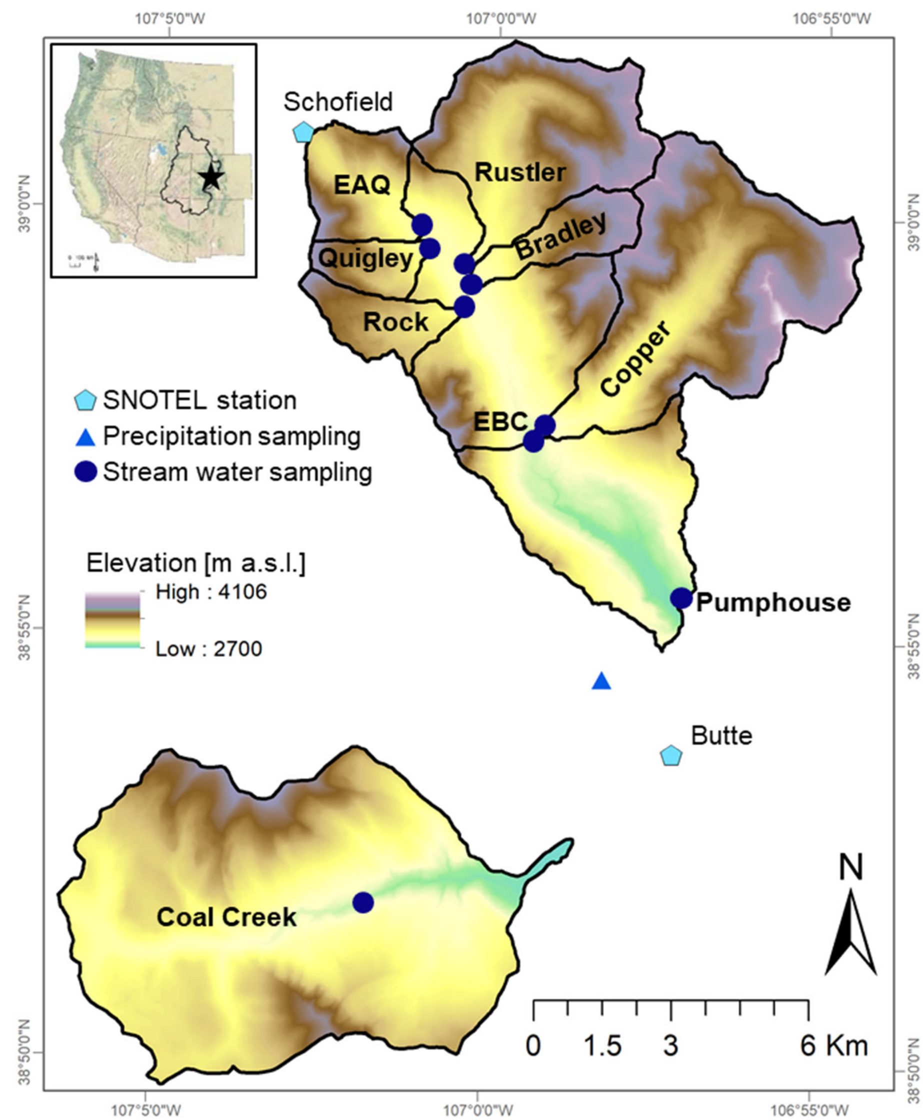

Figure 1 Location of stream water and precipitation sampling as well as the SNOTEL stations in the study area. Name, boundaries and elevation distribution of all nine catchments shown. Upper left insert shows the Upper Colorado Basin (black line) and the East River (star) within the western US.

2.2 Analyses

2.2.1 Endmember splitting and mixing analysis

Based on the $\delta^{18}O$ data in precipitation and streamflow, we applied endmember splitting and mixing analyses (Kirchner and Allen, 2020). (Kirchner, 2019). We defined snow (P_S) and rain (P_R) as the two endmembers because of their distinct isotopic compositions with weighted averages of $\delta^{18}O_{PS}$ = -18.18 and $\delta^{18}O_{PR}$ = -6.90, respectively (Suppl. Fig. 3). We differentiated the temporal and catchment specific variations in snow and rainfall based on air temperature variations, precipitation, and ASO snow depth estimates provided by Carroll et al. (2022a) to estimate P_S and P_R volumes. Spatial variation of $\delta^{18}O$ was accounted for based on a isotope lapse rate of -0.16‰/100 m, derived from weekly sampling of snowfall along an elevation gradient (Carroll et al., 2022b). We separated the stream water during summer (July, August, and September) and non-summer (October to June) periods as the two output endmembers, Q_S and Q_{nS}, respectively. With this definition, the snowmelt peak runoff occurred during Q_{nS}, while Q_S covered the hydrograph recession, including the monsoon season (Suppl. Fig. 4). Precipitation isotope ratios were weighted by the respective precipitation sums, and the discharge isotope ratios were weighted by the flow volume at the sampling day.

We conducted the endmember splitting and mixing analyses for all available data from water-years 2015-2020, which when aggregated, approaches the long-term isotope mass balance. We also conducted the analyses for the individual years for all the catchments that had sufficient stream water isotope data available. For endmember mixing and splitting analyses, the water balance is assumed to be closed (Kirchner and Allen, 2020), because it implies that the catchment storage change is zero and that the ET sum is the difference between precipitation and catchment streamflow sums. For the inter-annual analyses this assumption might not be valid, so we focus our interpretation mostly on the long-term analyses.

2.2.2 Statistical analyses

As the catchment characteristics are highly cross correlated (Suppl. Fig. 1), we applied a rotated principle component analysis to extract four components that represented the variation of the following catchment characteristics: share of alpine and montane area, respectively, drainage density, topographic wetness index, catchment area, share of Mancos shale in catchment, average elevation, relief, average slope, average aspect, and tree cover density (Suppl. Table 1). For each of the four relative components, we picked the one catchment character that correlated the most with the individual components (Suppl. Fig. 2) to be a representative predictor. With these four representative predictors, we performed a multiple linear regression analysis and derived the relative importance of them to describe the spatial variance of endmember mixing and splitting results across the nine catchments.

3 Results: Snow and rain contributions to summer runoff and evapotranspiration

3.1 Spatial variability

Our endmember mixing analyses revealed that across all catchments (average ± standard deviation) snow provided 85% of total precipitation between 2015 and 2020, and thus was the dominant water source for Q_{nS} (94±3%), Q_S (90±1%) and ET (74±8%) (Table 1). Therefore, snowmelt was – relatively to the input volumes– overrepresented in Q and underrepresented in ET. Conversely, rainfall played a special role in sustaining ET fluxes during the summer. The fraction of rain and snow in Q_{nS} and Q_S across the catchments was well explained by the multiple linear regression analyses (r^2=0.78 and r^2=0.74, respectively) with the average catchment aspect being the main driver (Figure 2a). In more westerly exposed catchments, Q_S and Q_{nS} typically contained less rain ($Q_S \leftarrow P_R$, r=-0.79 and $Q_{nS} \leftarrow P_R$, r=-0.88, respectively, Figure 2e,f). This relationship is due to a greater ET dominance at westerly-exposed hillslopes, were summers are warmer and thus rain potentially evapotranspires shortly after it falls leading to less rainwater sourcing for streamflow in western facing catchments. The share of snow and rain in ET ($ET \leftarrow P_R$) was generally more variable across the catchments. Multiple linear regression described its variation moderately well (r^2=0.63) with tree cover density explaining 34 % of the regression and aspect and drainage density explaining 27 and 24% of the variability respectively (Figure 2a). In general, there was a higher share of snow in ET ($ET \leftarrow P_S$) in catchments with higher tree cover density (r=0.53, p=0.15), which explains much of the inter-catchment variation of the endmember mixing results. Consequently, Q_{nS} and Q_S had a lower share of snow with increasing tree cover density. Neither the catchment's drainage density nor size was a good predictor of the snow and rain contributions to the outflows.

Table 1 End member mixing and splitting results (± standard error) for each catchment and the average (±SD) over all nine catchments. For endmember mixing, only rainfall is shown, as snowfall source is the difference to 100%. Arrows indicate for end-member mixing the relative share of an endmember (rain or snow) in one of the three defined outflows (summer discharge, Q_S, non-summer discharge, Q_{nS}, or evapotranspiration, ET) and for end-member splitting the relative share of an endmember (rain or snow) to become one of the three defined outflows (summer discharge, Q_S, non-summer discharge, Q_{nS}, or evapotranspiration, ET).

	End-member mixing			End-member splitting					
	Q_S←Rain	Q_{nS}←Rain	ET←Rain	Rain→Q_S	Rain→Q_{nS}	Rain→ET	Snow→Q_S	Snow→Q_{nS}	Snow→ET
Quigley	12 (±4) %	8 (±4) %	18 (±5) %	5% (±2)	24 (±12) %	71 (±4) %	6 (±1) %	43 (±4) %	50 (±5) %
Rock	13 (±4) %	7 (±4) %	27 (±9) %	6 (±2) %	25 (±15) %	69 (±6) %	7 (±1) %	60 (±6) %	33 (±6) %
Bradley	4 (±4) %	4 (±4) %	31 (±9) %	4 (±5) %	12 (±13) %	84 (±4) %	18 (±2) %	50 (±4) %	32 (±5) %
EAQ	10 (±4) %	9 (±4) %	14 (±13) %	12 (±5) %	53 (±25) %	35 (±6) %	13 (±1) %	62 (±6) %	25 (±7) %
Rustlers	11 (±4) %	6 (±4) %	25 (±17) %	14 (±6) %	35 (±23) %	50 (±6) %	15% (±1)	66 (±6) %	19 (±7) %
Copper	8 (±4) %	5 (±4) %	38 (±13) %	10 (±5) %	17 (±14) %	73 (±4) %	21 (±2) %	56 (±4) %	23 (±6) %
EBC	9 (±4) %	6 (±4) %	25 (±6) %	11 (±5) %	14 (±11) %	75 (±3) %	20 (±2) %	40 (±3) %	40 (±4) %
Coal	10 (±4) %	7 (±4) %	20 (±4) %	4 (±1) %	19 (±13) %	78 (±4) %	5 (±1) %	43 (±4) %	51 (±4) %
PH	11 (±4) %	6 (±4) %	35 (±11) %	10 (±4) %	20 (±15) %	70 (±4) %	17 (±1) %	59 (±4) %	25 (±6) %
Avg.	10 (±3) %	6 (±1) %	26 (±8) %	8 (±4) %	24 (±13) %	67 (±15) %	13 (±6) %	53 (±9) %	33 (±12) %

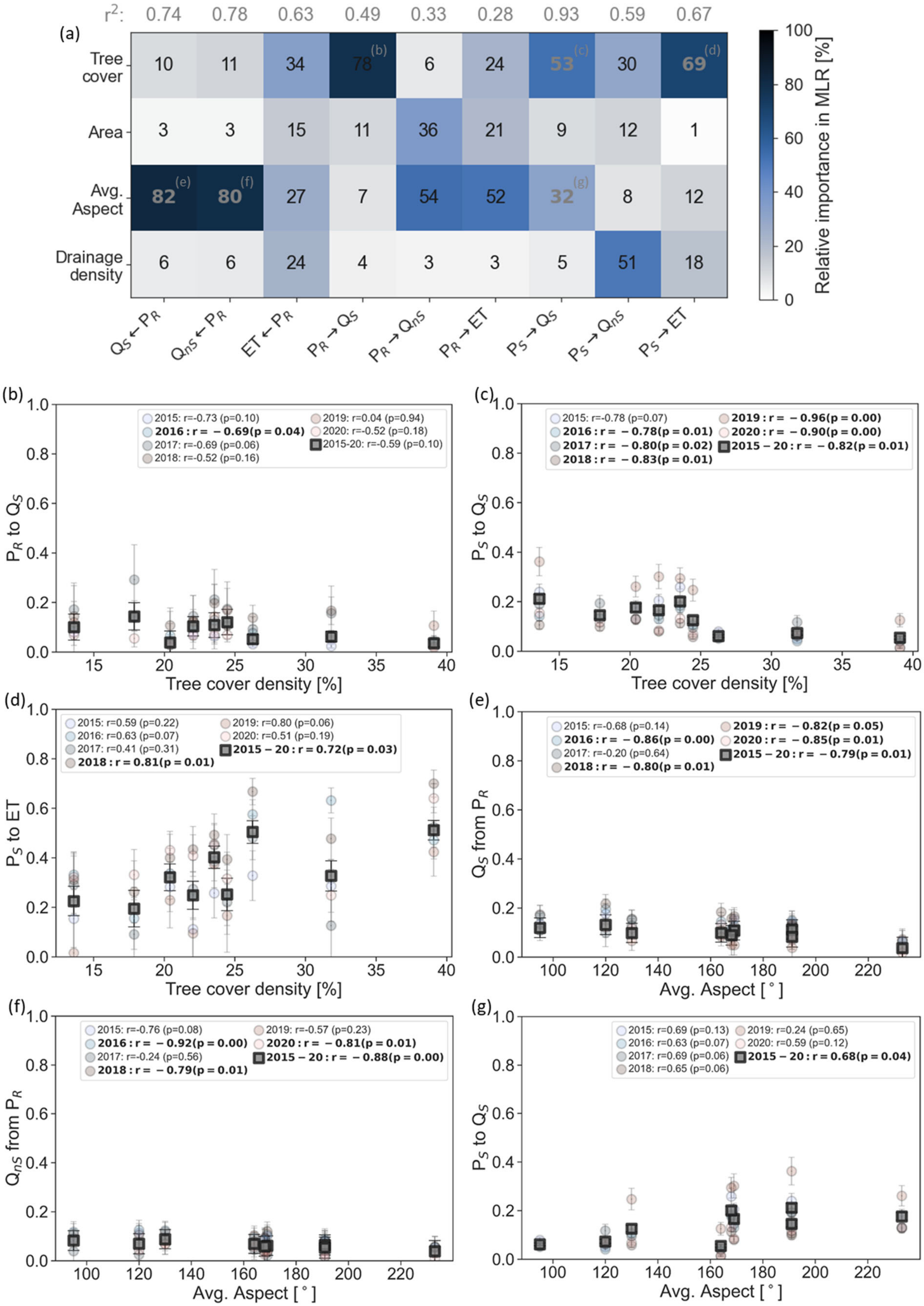

r²: 0.74 0.78 0.63 0.49 0.33 0.28 0.93 0.59 0.67
(a)
Tree cover
Area
Avg. Aspect
Drainage density
10 11 34 78 (b) 6 24 53 (c) 30 69 (d)
3 3 15 11 36 21 9 12 1
82 (e) 80 (f) 27 7 54 52 32 (g) 8 12
6 6 24 4 3 3 5 51 18
Q_S ← P_R
Q_nS ← P_R
ET ← P_R
P_R → Q_S
P_R → Q_nS
P_R → ET
P_S → Q_S
P_S → Q_nS
P_S → ET
Relative importance in MLR [%]
(b)
2015: r=-0.73 (p=0.10)
2016: r = −0.69(p = 0.04)
2017: r=-0.69 (p=0.06)
2018: r=-0.52 (p=0.16)
2019: r=0.04 (p=0.94)
2020: r=-0.52 (p=0.18)
2015-20: r=-0.59 (p=0.10)
P_R to Q_S
Tree cover density [%]
(c)
2015: r=-0.78 (p=0.07)
2016: r = −0.78(p = 0.01)
2017: r = −0.80(p = 0.02)
2018: r = −0.83(p = 0.01)
2019: r = −0.96(p = 0.00)
2020: r = −0.90(p = 0.00)
2015 − 20: r = −0.82(p = 0.01)
P_S to Q_S
Tree cover density [%]
(d)
2015: r=0.59 (p=0.22)
2016: r=0.63 (p=0.07)
2017: r=0.41 (p=0.31)
2018: r = 0.81(p = 0.01)
2019: r=0.80 (p=0.06)
2020: r=0.51 (p=0.19)
2015 − 20: r = 0.72(p = 0.03)
P_S to ET
Tree cover density [%]
(e)
2015: r=-0.68 (p=0.14)
2016: r = −0.86(p = 0.00)
2017: r=-0.20 (p=0.64)
2018: r = −0.80(p = 0.01)
2019: r = −0.82(p = 0.05)
2020: r = −0.85(p = 0.01)
2015 − 20: r = −0.79(p = 0.01)
Q_S from P_R
Avg. Aspect [°]
(f)
2015: r=-0.76 (p=0.08)
2016: r = −0.92(p = 0.00)
2017: r=-0.24 (p=0.56)
2018: r = −0.79(p = 0.01)
2019: r=-0.57 (p=0.23)
2020: r = −0.81(p = 0.01)
2015 − 20: r = −0.88(p = 0.00)
Q_nS from P_R
Avg. Aspect [°]
(g)
2015: r=0.69 (p=0.13)
2016: r=0.63 (p=0.07)
2017: r=0.69 (p=0.06)
2018: r=0.65 (p=0.06)
2019: r=0.24 (p=0.65)
2020: r=0.59 (p=0.12)
2015 − 20: r = 0.68(p = 0.04)
P_S to Q_S
Avg. Aspect [°]

Figure 2 (a) Relative importance of a multiple linear regression (MLR) model to explain variability of endmember mixing and splitting results. Bold grey numbers indicate regression parameters with p-values < 0.1. The individual relationships for parameters with significant correlations are shown in inserts (b to g). The r^2 of the regression models explaining the variation of the endmember mixing and splitting results across the catchments are shown in grey above each column.

Our endmember splitting results show that most rain was to partition into ET (67±15%, P_R→ET), while only a small fraction (8±4%) of the summer rainfall became Q_S (P_R→Q_S), and that 24±13% of rain left the catchments via Q_{nS} (P_R→Q_{nS}) (Table 1). In contrast, only 33±12% of snow ended up as ET (P_S→ET) while most of the snow became Q_{nS} (53±9%, P_S→Q_{nS}) and to lesser extent Q_S (13±6%, P_S→Q_S).

Vegetation cover provided a primary control on the differences in endmember splitting across the catchments. Our results show that tree cover density accounts 78% relative importance in a multiple linear regression describing how much of rainfall partitions to Q_S across the different catchments (Figure 2a,b). The share of rain becoming Q_{nS} was mainly determined by the catchment aspect and the catchment size, but the predictive power of the multiple linear regression model was low (r^2=0.33), which makes interpretations uncertain. The coefficient of determination was also low for the regression analysis to explain the variation in the fraction of rainfall becoming ET (r^2=0.28) across catchments. Aspect accounted for most (52%) of the relative importance in this regression, and tree cover density and catchment size 24% and 21%, respectively, while drainage density did not play a role (Figure 2a).

The multiple regression models for the spatial variation of the snow endmember splitting showed much better coefficients of variation than for the rainfall splitting. The share of snow that became Q_S was well described (r^2=0.93) with tree cover density as the most important predictor (53%) and average aspect explaining 33% of the variation. With increasing tree cover density, snow was less likely to become Q_S (r=-0.82, Figure 2c), because more snow ended up in ET (r=0.72, Figure 2d). Therefore, tree cover density was the most important predictor (69%) in the regression model explaining the variability of snow becoming ET. Aspect played a secondary role for the snow contributions to Q_{nS} (r=0.68, Figure 2g). Drainage density explained some of the variability in snowfall becoming Q_{nS}, however, this correlation was weak and not statistically significant.

In addition to the catchment characteristics, hydrometeorological variations across the catchments also impacted the endmember mixing and splitting results. We found that as ET magnitude increases, a greater percentage of that ET was sourced from snow (significant for 2015, 2016, 2019, 2020, Figure 3a), a result explained by belowground snowmelt storage subsiding summertime ET during precipitation limited conditions. This dependency of ET on snowmelt contributions was further supported by the observed trend that in catchments with more snowfall, more of the snow became ET during low-snow years (2015, 2016, 2018, Figure 3b).

In general, higher ET in catchments led to a greater percentage of snow becoming ET (Figure 3g), and less snow ending up in Q_{nS} (Figure 3e) which underlies the importance of snow sources and spatial variability for ET fluxes. There was no correlation between the rainfall contributions to ET and inter-annual variation of ET sums, which shows that most of the rainfall was generally – independently of the evaporative demand – becoming ET. The importance of monsoon rains in sustaining Q_S was also documented: catchments with higher rainfall sums not only resulted in higher Q_S, but also resulted in more snow becoming Q_S (Figure 3d) which indicated that snow stored in the subsurface was mobilized by summer rainfall and thus contributing to summer streamflow. Outside of summers, more of Q_{nS} was sourced by snow as flow increased (Figure 3f).

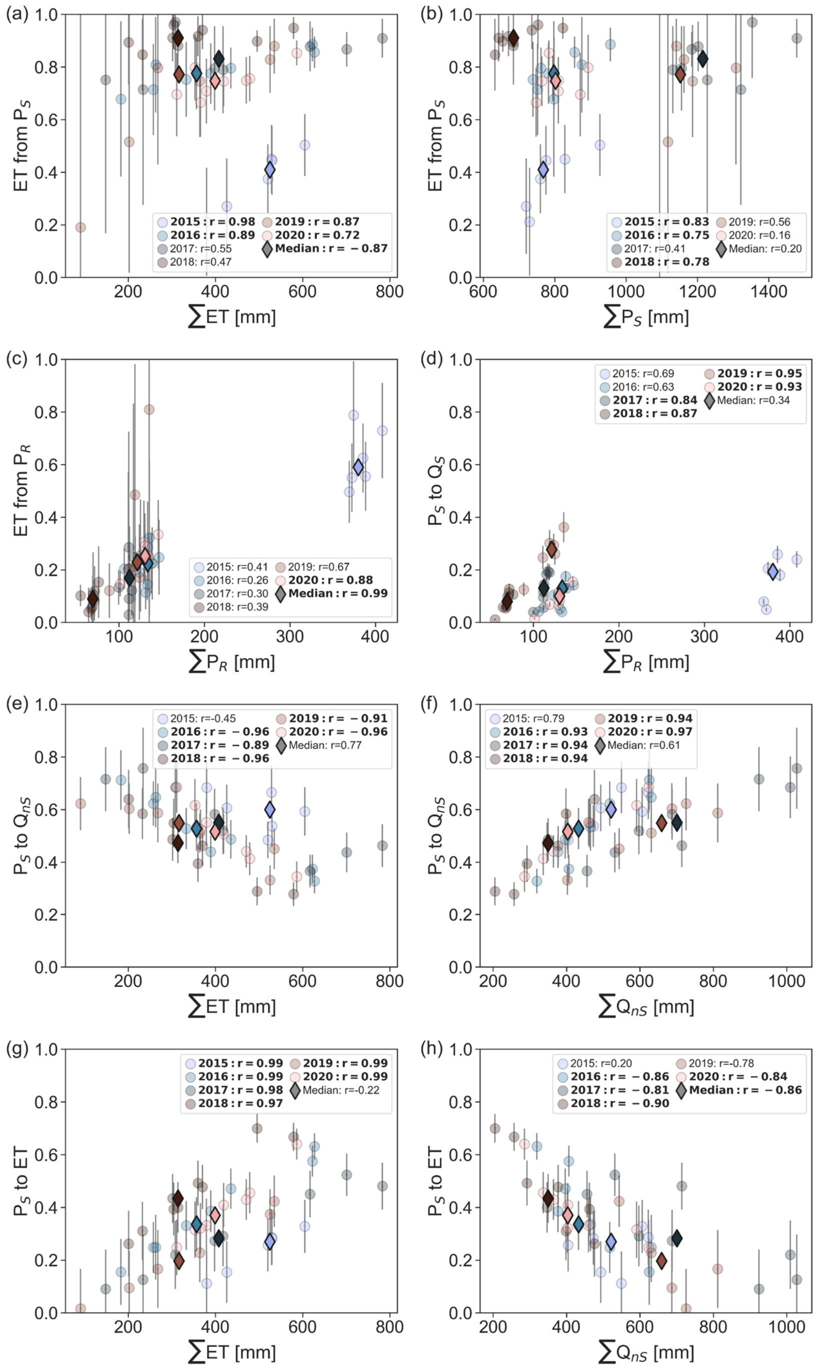

Figure 3 Endmember mixing (a – c) and endmember splitting (d – h) results as a function of hydrometric data: annual sums of evapotranspiration (ET), snowfall (P_S), rainfall (P_R), and non-summer streamflow (Q_{nS}). Shown are results from individual catchments and years (circles and color coded) as well as median values across all catchments for individual years (diamonds). Correlation coefficients are given in the legend and bold font indicates significant correlations ($p<0.05$). Circles represent variability across catchments for individual years and diamonds represent variability between different years averaged over the catchments.

3.2 Temporal variability

The spatial relationships between endmember mixing and splitting results and catchment characteristics were relatively constant in time (see half-transparent circles in Figure 2 b-g). However, there are inter-annual dynamics in the partitioning that stem from the hydrometeorological conditions. For example, in years with higher P_R, more ET was sourced from rain (r=0.99, Figure 3c). Endmember splitting further showed that there was also a trend of more rainfall becoming ET as rainfall and ET increased (r=0.63, p=0.18 and r=0.73, p=0.10, respectively), leaving less rain to support streamflow. Wetter years with higher Q_{nS} resulted in more snow becoming Q_{nS} (Figure 3f) and a lower fraction of snow ended up as ET (Figure 3h).

Not surprisingly, there was a trend towards more snow in both Q_S and Q_{nS} (r=0.77, p=0.08 and r=0.75, p=0.09, respectively) for years with higher SWE_{max}, but the splitting of snow into ET and Q was independent of the annual SWE_{max}.

4 Discussion

Similar to the initial endmember splitting and mixing work by Kirchner & Allen (2020) for the humid Watershed 3 at Hubbard Brook Experimental Forest, our analyses shows that inter-seasonal water storage is an integral part of storage and release of water in headwater mountainous catchments. However, the snow dominance of the water balance in the UCRB and the resulting hydrograph led to different precipitation partitioning dynamics than for Hubbard Brook.

Our multi-catchment approach permitted inference of controls on the spatial variability in precipitation partitioning in mountainous regions. We found that aspect and tree cover density were the main driver of the spatial variability. More SW exposed catchments had a higher share of snow in their streamflow, which cannot be explained by spatial variation in snow, because SW exposed catchments had lower snowpack volumes than the NE exposed ones (Carroll et al., 2022a). Thus, the influence of aspect on the snowmelt timing and the consequences for the runoff generation and the timing of the transpiration onset seems to govern the partitioning. As more of the snowmelt happens earlier in catchments with more hillslopes exposed to the SW, the snowmelt drains towards the stream and groundwater and is therefore less likely to get evapotranspired (Barnhart et al., 2016; Molotch et al., 2009). By the time snowmelt happens at NE exposed hillslopes evapotranspiration rates are already higher, which then changes the partitioning of the snow towards higher losses via ET. The variability in rain and snow partitioning has implications for critical watershed functions, such as water delivery, drought resilience, and nitrogen export, and our results help to explain potential sources and mechanisms of these observed functions (Newcomer et al., 2021; Wainwright et al., 2022).

Our tracer based results for head-water catchments indicate that 90% of runoff is sourced by snow, which is the upper limit of the water balance based estimates for various locations across the western US (Li et al., 2017). Specifically for the East River, our findings corroborate hydrologic modeling results that showed that most rain gets evapotranspired, and little rain becomes runoff to the East River (Carroll et al., 2020b). Our estimate of ~7% of total Q stemming from rain for the East River at Pumphouse is within the range of modeled estimates (~10%, Carroll et al., 2020b). Our findings support ET source water estimates from particle tracking simulations, which indicated that ET of a forested hillslope in the East River catchment was to large parts sourced by snowmelt (Maxwell et al., 2019). Their simulations indicated that between Mid-June to September, rainfall became a more important ET source, which aligns with our finding that most of the rainfall is evapotranspired. The importance of snow for transpiration is further supported by isotope-based plot-scale ecohydrological studies in the East River (Berkelhammer et al., 2020) and across Switzerland (Allen et al., 2019). Berkelhammer (2020) showed that rain becomes a more important plant water source as it infiltrates into the shallow soil layers and is subsequently taken up by trees in the later growing season. While these isotope studies and tracer-based modeling work (Brinkmann et al., 2018; Sprenger et al., 2018) at the plot-scale indicated that trees take up relatively old (e.g., snowmelt) water, our catchment-wide isotope water balances revealed that these ecohydrological processes are generally relevant for storage and release of water at the catchment scale. Our findings underlie both the importance of snow water uptake by plants and also the quick turnover time of rainfall becoming ET, as two-thirds of the rainfall was evapotranspired according to our endmember splitting analyses.

Due to ecohydrological feedbacks between subsurface water storage and root water uptake, vegetation cover played a crucial role in our study to explain partitioning of snow and rainfall into Q and ET. We infer that with higher tree cover density, the rooting system will be more efficient in extracting potentially deeper soil layers where snowmelt is being stored during the summer, sustaining the summertime evaporative demand. Carroll et al. (2018) found that the groundwater fraction in the streamflow decreases with tree cover density across East River catchments. Since snow is the main source of groundwater recharge in the East River, our results support the finding that snow contributions to runoff decreases with tree cover density. Our multi-year analysis shows that this relationship between tree cover density and runoff processes is relatively constant in time. A low-to-no-snow future in which the water deficit is not compensated by increased rainfall would therefore pose a potential drought stress for plants, higher risk of fires, and changes to water and chemical exports that are currently adapted to inter-seasonal water storage (Newcomer et al., 2021).

The higher share of snow in ET with increased ET sum that we observed can explain the “drought-paradox” (Teuling et al., 2013), that ET increases during drought periods. Since ET is sourced in large part (60 – 80 %) from snow in the UCRB, a dry summer with reduced monsoon rainfall will have relatively little impact on ET rates. Conversely, greater monsoon rains during summer may result in a higher fraction of P_R partitioning to ET, which lowers snow water losses to the atmosphere and potentially helps retain subsurface storage. However, an increased ET flux leads to a higher share of snow in ET, which can cause a strong water deficiency in a warmer low-snow to no-snow future with increased ET demand (Milly and Dunne, 2020; Woodburn et al., 2021).

Our endmember mixing and splitting results highlight that climate projections will need to account for ecohydrological interactions between shifts in snow volumes, the timing of melt and the resulting soil and bedrock moisture dynamics that impact plant water use during climatic extremes (e.g., Mastrotheodoros et al., 2020). Despite uncertainties associated with the spatial and temporal variability in snow and rain volumes and stable isotope ratios (Carroll et al., 2022a), these two endmembers are isotopically strongly dissimilar, and thus, the observed patterns have been consistent both in space (across the catchments) and in time (individual years and long-term mass balance). Endmember mixing and splitting has therefore shown to be highly informative for catchment scale processes, which helps benchmark hydrological models and assess sources and mechanisms for changing watershed conditions.

5 Conclusion

Our results show how stable isotopes of water can inform our perspective of catchment scale hydrological partitioning and mass balance components in snow-dominated mountainous regions. Observed partitioning of snow and rain into either ET or summer and non-summer Q highlighted the importance of snowmelt contributions to catchment storage that sustain not only the seasonal streamflow, but also evaporative demand in the vegetated headwaters. Variability across the nine catchments showed the influence of vegetation on mixing and splitting, as higher tree cover density resulted in higher snow water loss to the atmosphere and less snow contributing to streamflow. Two-thirds of the summer rainfall was evapotranspired, while only ~10 % of the summer streamflow was from rainfall. We therefore conclude that in a future low-snow mountain environment, the evaporative demand of the forested catchments will only be met with a pronounced increase in rainfall to overcome water scarcity for ecosystem and anthropogenic use. Our catchment scale isotope mass balance work can help upscale plot-scale observations and test hydrological models, which will improve mechanistic process representation of rain/snow partitioning under future climate regimes.

Acknowledgements

This work was supported by the US Department of Energy Office of Science under contract DE-AC02-05CH11231 as part of Lawrence Berkeley National Laboratory Watershed Function Science Focus Area. We would like to express appreciation to the Rocky Mountain Biological Laboratory for handling US Forest Service permitting.

Author contributions

MS conducted the data analysis, made graphs, and wrote the initial draft of the manuscript; WB, WN, CB, MB, and RWHC contributed to data gathering in the field and laboratory; RWHC, MN, and KHW contributed to data curation and analysis; JDF and ERSW contributed to data analysis and interpretation; RWHC, JDF, SSH, MN, and KHW contributed to manuscript revisions.

Competing interests

The authors declare no competing interests.

Data availability

The endmember mixing and splitting code (Kirchner, 2019) and the data on streamflow (Carroll et al., 2020a; Newcomer et al., 2022) and stable isotope data (Carroll et al., 2021; Williams et al., 2020) are freely and publicly available online on the DOE ESS-DIVE data repository as cited.

References

Allen, S. T., Kirchner, J. W., Braun, S., Siegwolf, R. T. W. and Goldsmith, G. R.: Seasonal origins of soil water used by trees, Hydrol. Earth Syst. Sci., 23(2), 1199–1210, doi:10.5194/hess-23-1199-2019, 2019.

Barnhart, T. B., Molotch, N. P., Livneh, B., Harpold, A. A., Knowles, J. F. and Schneider, D.: Snowmelt rate dictates streamflow, Geophys. Res. Lett., 43(15), 8006–8016, doi:10.1002/2016GL069690, 2016.

Berkelhammer, M., Still, C. J., Ritter, F., Winnick, M., Anderson, L., Carroll, R., Carbone, M. and Williams, K. H.: Persistence and Plasticity in Conifer Water-Use Strategies, J. Geophys. Res. Biogeosciences, 125(2), 1, doi:10.1029/2018JG004845, 2020.

Brinkmann, N., Seeger, S., Weiler, M., Buchmann, N., Eugster, W. and Kahmen, A.: Employing stable isotopes to determine the residence times of soil water and the temporal origin of water taken up by Fagus sylvatica and Picea abies in a temperate forest, New Phytol., 219(4), 1300–1313, doi:10.1111/nph.15255, 2018.

Carroll, R. and Willlams, K. H.: Discharge data collected within the East River for the LBNL Watershed Function Science Focus Area (water years 2015-2018), Watershed Funct. SFA, doi:10.21952/WTR/1495380, 2019.

Carroll, R., Newman, A., Beutler, C. and Williams, K. H.: Stream discharge data collected within the East River, Colorado for the Lawrence Berkeley National Laboratory Watershed Function Science Focus Area (water year 2019-2020, present), Watershed Funct. SFA, doi:10.15485/1779721, 2020a.

Carroll, R. W. H., Bearup, L. A., Brown, W., Dong, W., Bill, M. and Willlams, K. H.: Factors controlling seasonal groundwater and solute flux from snow-dominated basins, Hydrol. Process., 32(14), 2187–2202, doi:10.1002/hyp.13151, 2018.

Carroll, R. W. H., Gochis, D. and Williams, K. H.: Efficiency of the Summer Monsoon in Generating Streamflow Within a Snow - Dominated Headwater Basin of the Colorado River Geophysical Research Letters, Geophys. Res. Lett., 47(23), e2020GL090856, doi:10.1029/2020GL090856, 2020b.

Carroll, R. W. H., Brown, W., Newman, A., Beutler, C. and Williams, K. H.: East River Watershed Stable Water Isotope Data in Precipitation, Snowpack and Snowmelt 2016-2020, Watershed Funct. SFA, doi:10.15485/1824223, 2021.

Carroll, R. W. H., Deems, J., Sprenger, M., Maxwell, R., Brown, W., Newman, A., Beutler, C. and Williams, K. H.: Modeling Snow Dynamics and Stable Water Isotopes Across Mountain Landscapes, Earth Sp. Sci. Open Arch., doi:10.1002/essoar.10510911.1, 2022a.

Carroll, R. W. H., Deems, J., Maxwell, R., Sprenger, M., Brown, W., Newman, A., Beutler, C., Bill, M., Hubbard, S. S. and Williams, K. H.: Variability in observed stable water isotopes in snowpack across a mountainous watershed in Colorado, Hydrol. Process., 2022b.

Gaskill, D. L., Mutschler, F. E. and Kramer, J. H.: Geologic map of the Gothic Quadrangle, Gunnison County, Colorado., 1991.

Hock, R., Rasul, G., Adler, C., Cáceres, B., Gruber, S., Hirabayashi, Y., Jackson, M., Kääb, A., Kang, S., Kutuzov, S., Milner, A., Molau, U., Morin, S., Orlove, B. and Steltzer, H.: High Mountain Areas, in IPCC Special Report on the Ocean and Cryosphere in a Changing Climate, edited by H.-O. Pörtner, D. C. Roberts, V. Masson-Delmotte, P. Zhai, M. Tignor, E. Poloczanska, K. Mintenbeck, A. Alegría, M. Nicolai, A. Okem, J. Petzold, B. Rama, and N. M. Weyer., 2019.

Hubbard, S. S., Williams, K. H., Agarwal, D., Banfield, J., Beller, H., Bouskill, N., Brodie, E., Carroll, R., Dafflon, B., Dwivedi, D., Falco, N., Faybishenko, B., Maxwell, R., Nico, P., Steefel, C., Steltzer, H., Tokunaga, T., Tran, P. A., Wainwright, H. and Varadharajan, C.: The East River, Colorado, Watershed: A Mountainous Community Testbed for Improving Predictive Understanding of Multiscale Hydrological–Biogeochemical Dynamics, Vadose Zo. J., 17(1), 180061, doi:10.2136/vzj2018.03.0061, 2018.

Ikeda, K., Rasmussen, R., Liu, C., Newman, A., Chen, F., Barlage, M., Gutmann, E., Dudhia, J., Dai, A., Luce, C. and Musselman, K.: Snowfall and snowpack in the Western U . S . as captured by convection permitting climate simulations : current climate and pseudo global warming future climate, Clim. Dyn., 57(7), 2191–2215, doi:10.1007/s00382-021-05805-w, 2021.

Immerzeel, W. W., Lutz, A. F., Andrade, M., Bahl, A., Biemans, H., Bolch, T., Hyde, S., Brumby, S., Davies, B. J., Elmore, A. C., Emmer, A., Feng, M., Fernández, A., Haritashya, U., Kargel, J.

S., Koppes, M., Kraaijenbrink, P. D. A., Kulkarni, A. V, Mayewski, P. A., Pacheco, P., Painter, T. H., Pellicciotti, F., Rajaram, H., Rupper, S., Sinisalo, A., Shrestha, A. B., Viviroli, D., Wada, Y., Xiao, C., Yao, T. and Baillie, J. E. M.: Importance and vulnerability of the world ' s water towers, Nature, 577(May 2019), doi:10.1038/s41586-019-1822-y, 2020.

Kirchner, J. W.: EndSplit, EnviDat, doi:10.16904/envidat.91., 2019.

Kirchner, J. W. and Allen, S. T.: Seasonal partitioning of precipitation between streamflow and evapotranspiration, inferred from end-member splitting analysis, Hydrol. Earth Syst. Sci., 24(1), 17–39, doi:10.5194/hess-24-17-2020, 2020.

Li, D., Wrzesien, M. L., Durand, M., Adam, J. and Lettenmaier, D. P.: How much runoff originates as snow in the western United States, and how will that change in the future?, Geophys. Res. Lett., 44, 6163–6172, doi:10.1002/2017GL073551, 2017.

Mastrotheodoros, T., Pappas, C., Molnar, P., Burlando, P., Manoli, G., Parajka, J., Rigon, R., Szeles, B., Bottazzi, M., Hadjidoukas, P. and Fatichi, S.: More green and less blue water in the Alps during warmer summers, Nat. Clim. Chang., 10(2), 155–161, doi:10.1038/s41558-019-0676-5, 2020.

Maxwell, R. M., Condon, L. E., Danesh-Yazdi, M. and Bearup, L. A.: Exploring source water mixing and transient residence time distributions of outflow and evapotranspiration with an integrated hydrologic model and Lagrangian particle tracking approach, Ecohydrology, 12(1), e2042, doi:10.1002/eco.2042, 2019.

Milly, P. C. D. and Dunne, K. A.: Colorado River flow dwindles as warming-driven loss of reflective snow energizes evaporation, Science (80-.)., 367(6483), 1252–1255, doi:10.1126/science.aax0194, 2020.

Molotch, N. P., Brooks, P. D., Burns, S. P., Litvak, M., Monson, R. K., Mcconnell, J. R. and Musselman, K.: Ecohydrological controls on snowmelt partitioning in mixed-conifer sub-alpine forests, Ecohydrology, 2, 129–142, doi:10.1002/eco.48, 2009.

Musselman, K. N., Addor, N., Vano, J. A. and Molotch, N. P.: Winter melt trends portend widespread declines in snow water resources, Nat. Clim. Chang., 11, 418–424, doi:10.1038/s41558-021-01014-9, 2021.

Newcomer, M. E., Bouskill, N. J. and Wainwright, H.: Hysteresis Patterns of Watershed Nitrogen Retention and Loss Over the Past 50 years in United States Hydrological Basins Global Biogeochemical Cycles, , 1–28, doi:10.1029/2020GB006777, 2021.

Newcomer, M. E., Williams, K. W. and R.W.H, C.: Machine Learning Assisted Gap-Filled Discharge Data for the East River Community Watereshed for Water Years 2014-2021, Watershed Funct. SFA, 2022. https://www.dropbox.com/s/gd9jxv4f1x7blao/All_RF_Wide.csv?dl=0 (Upload to https://ess-dive.lbl.gov/ in progress and DOI fill follow)

Peel, M. C., Finlayson, B. L. and Mcmahon, T. A.: Updated world map of the Koeppen-Geiger climate classification, Hydrol. Earth Syst. Sci., 11, 1633–1644, doi:10.5194/hess-11-1633-2007, 2007.

Sprenger, M., Tetzlaff, D., Buttle, J., Laudon, H. and Soulsby, C.: Water ages in the critical zone of long-Term experimental sites in northern latitudes, Hydrol. Earth Syst. Sci., 22(7), 3965–3981, doi:10.5194/hess-22-3965-2018, 2018.

Teuling, A. J., Van Loon, A. F., Seneviratne, S. I., Lehner, I., Aubinet, M., Heinesch, B., Bernhofer, C., Grünwald, T., Prasse, H. and Spank, U.: Evapotranspiration amplifies European summer drought, Geophys. Res. Lett., 40(10), 2071–2075, doi:10.1002/grl.50495, 2013.

Uhlemann, S., Dafflon, B., Wainwright, H. M., Williams, K. H., Minsley, B., Zamudio, K., Carr, B., Falco, N., Ulrich, C. and Hubbard, S.: Surface parameters and bedrock properties covary across a mountainous watershed: Insights from machine learning and geophysics, Sci. Adv., 8(12), 1–16, doi:10.1126/sciadv.abj2479, 2022.

Wainwright, H. M., Uhlemann, S., Franklin, M., Falco, N., Bouskill, N. J., Newcomer, M. E., Dafflon, B., Siirila-woodburn, E. R., Minsley, B. J. and Williams, K. H.: Watershed zonation through hillslope clustering for tractably quantifying above- and below-ground watershed heterogeneity and functions, Hydrol. Earth Syst. Sci., 429–444, doi:10.5194/hess-26-429-2022, 2022.

Williams, K. H., Beutler, C. A., Bill, M., Brown, W., Newman, A. W. and Versteeg, R.: Stable Water Isotope Data for the East River Watershed, Colorado. Watershed Function SFA, ESS-DIVE Repos., doi:10.15485/1668053, 2020.

Woodburn, E. R. S.-, Rhoades, A. M., Szinai, J., Tague, C., Nico, P. S. and Huning, L. S.: A low-to-no snow future and its impacts on water resources in the western United States, Nat. Rev. Earth Environ., 2, 800–819, doi:10.1038/s43017-021-00219-y, 2021.